1. Agency Use Only (Leave blank).	2. Report Date.	3. Report Type and Dates Covered.
	1994	Final - Book Contribution

4. Title and Subtitle.
Carbonate Microfabrics
Permeability Characteristics of Continental Slope and Deep-Water Carbonates from a Microfabric Perspective

5. Funding Numbers.
Program Element No. 61153N
Project No. 03202
Task No. 030
Accession No. DN255014
Work Unit No. 13610C

6. Author(s).
Lavoie, D. L. and W. Bryant

7. Performing Organization Name(s) and Address(es).
Naval Research Laboratory
Marine Geosciences Division
Stennis Space Center, MS 39529-5004

8. Performing Organization Report Number.
Front. in Sed. Geology, Carbonate Microfabrics, pp. 117-128

9. Sponsoring/Monitoring Agency Name(s) and Address(es).
Naval Research Laboratory
Stennis Space Center, MS 39529-5004

10. Sponsoring/Monitoring Agency Report Number.
NRL/BC004-90-361

11. Supplementary Notes.

12a. Distribution/Availability Statement.
Approved for public release; distribution is unlimited.

12b. Distribution Code.

13. Abstract *(Maximum 200 words).*

Permeability, the rate at which fluids move through a porous medium, affects the consolidation and reduction in porosity of a sediment with time and overburden pressure. Most marine clays consist of smectites and illites that are fine-grained and platey. In contrast, carbonate sediments are composed of multishaped, multisized components. In general, clay-rich sediments consolidate to lower porosities and are less permeable that carbonates at given overburden pressures. This difference is related to microfabric.

Numerous samples recovered from the continental slope to midocean depths were consolidated in the laboratory, and permeabilities were determined directly by using falling head permeameters and indirectly by consolidation theory. In the marine clays, porosity values ranged between 1 x 10^{-10} cm/s. In contrast, carbonate sediments with porosities between 60 and 40% had permeabilities that ranged between 1 x 10^{-4} and 1 x 10^{-7} cm/s. Sediments with varying percentages of carbonate content, but with a matrix of clay particles, fall within the same range as the clays. At given porosities, permeabilities within the carbonate sediments are determined by microfabric. For example, grain-supported samples have a higher permeability (1 x 10^{-4} cm/s) than matrix-supported samples (1 x 10^{-5} and 1 x 10^{-6} cm/s). In general, matrix-supported carbonate sediments composed of aragonite needles have higher permeabilities (1 x 10^{-5} cm/s) than matrix-supported sediments of low-magnesian calcite composed predominately of coccoliths (1 x 10^{-6} cm/s). Analysis of scanning and transmission electron micrographs of carbonate and clayey sediments confirm the more open microstructure of carbonate sediments as opposed to the more evenly distributed but smaller sized clay micropores.

14. Subject Terms.	15. Number of Pages.
Geoacoustics; Penetration; Sedimentology; Permeability; Penetrometers, Geotechnical Properties	12
	16. Price Code.

17. Security Classification of Report.	18. Security Classification of This Page.	19. Security Classification of Abstract.	20. Limitation of Abstract.
Unclassified	Unclassified	Unclassified	SAR

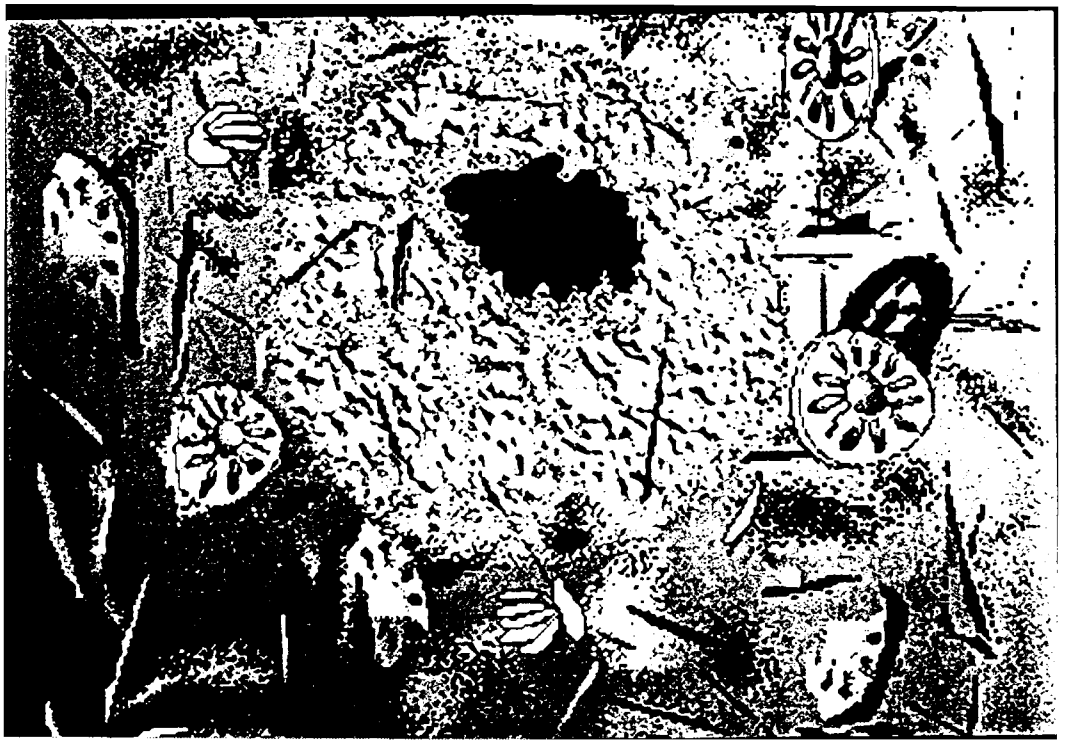

OVERVIEW

Recent Slope and Deep-Water Carbonates

Dawn L. Lavoie

Carbonate slopes may be categorized in two ways: as by-pass slopes, those on which sediment is transported from shallower to deeper water without significant deposition on the slope itself; or as accretionary slopes of gentle inclination, where the slopes merge gradually with the basin as sediment is deposited on the lower slope. On both types of carbonate slopes, in shallow and midwater depths, bank-derived aragonite and magnesian calcite are mixed with *in situ* low-magnesian calcite and aragonite. The resulting sediment is termed periplatform sediment (Schlager and James, 1978). These periplatform sediments differ from deep-water oozes because of the heterogeneity of various constituent particles and in the large component of reef-derived debris. Typical constituents of periplatform sediments include mollusc fragments, algal remnants, pteropods, coccoliths, foraminifers, sponge spicules, rhabdoliths, aragonite needles, pellets, and shell debris. In contrast, deep-water carbonate sediments tend to be more homogeneous with fewer types of particles, since most of the shelf-derived components are missing. The predominant deep-water carbonate constituents are planktonic foraminifers and nannofossils of stable, low-magnesian calcite, which produces carbonate skeletons that tend to form oozes. Correspondingly, the fabric of deep-water carbonate sediments is less complicated than that of periplatform sediments. Not discussed in this section are the carbonate turbidites, mainly because they have not been sufficiently studied.

Deep-sea carbonate deposits often grade abruptly into carbonate-poor sediments, such as red clays or siliceous oozes. This loss of carbonate begins at a depth at which the rate of carbonate sedimentation equals the rate of carbonate dissolution. This carbonate compensation depth (CCD) for calcite occurs at about 5000 m in the Atlantic (Blatt et al., 1980). Below the CCD, the rate of dissolution exceeds the rate of deposition, and carbonate sediments cease to accumulate. Above the CCD, at about 1000 m in the Atlantic, an aragonite compensation depth exists, below which aragonite accumulations are rare, except where they are produced in specialized seep environments. The chapters in this section span depths from above the aragonite compensation depth to below the carbonate compensation depth. The microfabric characteristics described in these chapters is a function of the depth of deposition, as well as the other various physical processes described by the authors.

The chapters in this section fall naturally into several subgroups (Fig. III.1). The first three chapters are primarily descriptive/interpretive. Wilber and Neumann describe the alteration of sedimentary facies by the precipitation of fine-grained magnesian calcite in the Bahamas. Roberts and coauthors describe special hydrocarbon seep environments on the Gulf Coast, where a unique community of chemosynthetic organisms have been found. The interaction between these organisms and the seeps produces large volumes of authigenic carbonates. Some of the authigenic carbonates described by Roberts et al. have been reproduced in the laboratory and are described by Busczynski and Chafetz in the following chapter.

The remaining chapters in this section are primarily geotechnical in nature. One objective of geotechnical research is to discover how the various geotechnical properties of carbonate sediments affect, or are affected by, geologic processes, and how these properties and processes are related to the microfabric of the sediment. Lavoie and Bryant span the arbitrary depth division between slope and deep-water carbonates and contrast the permeability of carbonate and clay sediments. Rack et al. are concerned with truly deep-water processes, the replacement of calcareous ooze by siliceous ooze. This process is influenced by external forcing

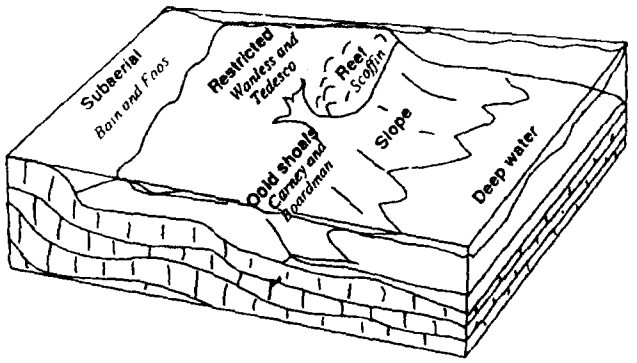

Figure III.1. Specialized deep-water environments discussed in Part III.

mechanisms (e.g., plate tectonics); therefore, these oozes contain significant paleoclimatic and oceanographic information that is reflected in measured geotechnical properties and microfabric. O'Brien et al. examine the role of preferred orientation of calcite in the velocity anisotropy of carbonate sediments, and Noorany reports on at the strength and compressibility of deep-sea carbonates.

A number of authors in this section and the previous one on shallow-water Recent carbonates have generated significant controversy in their use and misuse of carbonate terminology. For example, the following pairs of words are used synonymously by many authors in spite of their very different meanings: muddy and micritic sediments, texture and fabric, amorphous and noncrystalline, micrite and microcrystalline. Under fierce crossfire, we have left much of the authors' terminology as written and have devoted a portion of the Workshop Recommendations Chapter to sorting out and defining many of the commonly used and misused terms in this field. This glossary will reduce controversy among the carbonate specialists and provide guidance to those less familiar with this aspect of geology.

References

Blatt, H., G. Middleton, and R. Murray, 1980. Origin of Sedimentary Rocks, Prentice Hall, Inc., New Jersey, p. 474–476.

Schlager, W. and N.P. James, 1978. Low-magnesian calcite limestones forming at the deep-sea floor, Tongue of the Ocean, Bahamas, Sedimentology, v. 25, p. 675–702.

Acknowledgments

The Carbonate Microfabrics Symposium and Workshop and the preparation of this book for publication were supported by the Naval Oceanographic and Atmospheric Research Laboratory (NOARL), Stennis Space Center, MS; the College of Geosciences, Texas A&M University (TAMU); the Texas Institute of Oceanography, Galveston, Texas; and ARCO Oil and Gas Company, Plano, TX. We acknowledge the efforts of the session chairmen for preparing the programs for their respective sessions: Philip Sandberg, University of Illinois at Urbana, and Richard Bachman, Naval Ocean Systems Center (NOSC), San Diego, CA, for Recent, shallow-water carbonates; Conrad Neumann, University of North Carolina at Chapel Hill, and Richard Bennett, NOARL, for Recent, deep-water carbonates; Clyde Moore, Louisiana State University at Baton Rouge, and Steven Moshier, University of Kentucky at Lexington, for ancient, shallow-burial diagenetic microfabrics; and Robert Loucks, ARCO Oil and Gas Company at Plano, and Patrick Domenico, Texas A&M University, for ancient, deep-burial diagenetic microfabrics. We thank Kenneth Davis, Kathleen Locke, Scott Laswell, and Thomas Orsi, graduate students in the Oceanography Department at Texas A&M University, for their efforts during the symposium in assisting with the logistics and driving the transportation vehicles when they were needed. We are grateful to Kathleen Fischer for assisting with registration and various other tasks, including photography, during the symposium. Special thanks are due to Sandra Drews, secretary, Geological Section, Department of Oceanography, Texas A&M University, for organizing the mailings for the symposium, tracking responses, editing the program with abstracts booklet, and maintaining the files of correspondence during the preparation of this book.

Each of the chapters in this volume was reviewed by three technical critics and we thank the following persons for their constructive criticism: Richard Bachman, Naval Ocean Systems Center; Donald Bebout, University of Texas at Austin; Richard H. Bennett and Frederick Bowles, Naval Oceanographic and Atmospheric Research Laboratory; Richard Carlson, Texas A&M University; Albert Carozzi, University of Illinois at Urbana; Henry Chafetz, University of Houston; Philip Choquette, University of Colorado; Scott Cross, Duke University; Anna Dombrowski, Shell Western E&P, Houston; Jeff Dravis, Rice University; Kathleen Fischer, Naval Oceanographic and Atmospheric Research Laboratory; Robert Folk, University of Texas at Austin; John Grotzinger, Massachusetts Institute of Technology at Cambridge; Edwin Hamilton, Naval Ocean Systems Center; John D. Humphrey, University of Texas at Dallas; Ian Macintyre, Smithsonian Institute;

Isabell Montañez, University of California at Riverside; Steven Moshier, University of Kentucky at Lexington; Raymond Murray, University of Montana at Missoula; Conrad Neumann, University of North Carolina at Chapel Hill; Frank Rack, Texas A&M University; Perry Roehl, Trinity University at San Antonio; Duncan Sibley, Michigan State University at East Lansing; Terence Scoffin, University of Edinburgh; Eugene Shinn, U.S. Geological Survey at St. Petersburg; Niall Slowey, Texas A&M University; Lenore Tedesco, Indiana University - Purdue University at Indianapolis; Philip Valent, Naval Oceanographic and Atmospheric Research Laboratory; Harold Wanless, University of Miami; William C. Ward, University of New Orleans; Roy H. Wilkins, Hawaii Institute of Geophysics; James Lee Wilson, New Braunfels, Texas; and Donald Zenger, Pomona College.

We are especially grateful to the NOARL crew who did most of the production tasks normally completed by Springer-Verlag, New York. Sherryl A. Liddell was responsible for organizing the camera-ready setup of this book. In this role, she supervised the efforts of Linda H. Jenkins, who completed most of the literary editing, Maria H. Banker, who typeset the text and cheerfully made numerous changes, and Maryellen B. Turcotte, who was responsible for final page layout.

Finally we thank Arnold Bouma for his encouragement and support since the birth of the idea of putting together a symposium. His continued encouragement helped us through some rather difficult times when we were beginning to wonder if this book would ever see the light of day.

This publication has been approved for public release by NOARL with distribution unlimited. NOARL book contribution #004-01-361, program element #0601153N.

CHAPTER 9

Permeability Characteristics of Continental Slope and Deep-Water Carbonates from a Microfabric Perspective

Dawn L. Lavoie and William R. Bryant

Summary

Permeability, the rate at which fluids move through a porous medium, affects the consolidation and reduction in porosity of a sediment with time and overburden pressure. Most marine clays consist of smectites and illites that are fine-grained and platey. In contrast, carbonate sediments are composed of multishaped, multisized components. In general, clay-rich sediments consolidate to lower porosities and are less permeable than carbonates at given overburden pressures. This difference is related to microfabric.

Numerous samples recovered from the continental slope to midocean depths were consolidated in the laboratory, and permeabilities were determined directly by using falling head permeameters and indirectly by consolidation theory. In the marine clays, porosity values ranged between 75 and 40%, and permeability values ranged between 1×10^{-6} cm/s and 1×10^{-10} cm/s. In contrast, carbonate sediments with porosities between 60 and 40% had permeabilities that ranged between 1×10^{-4} and 1×10^{-7} cm/s. Sediments with varying percentages of carbonate content, but with a matrix of clay particles, fall within the same range as the clays. At given porosities, permeabilities within the carbonate sediments are determined by microfabric. For example, grain-supported samples have a higher permeability (1×10^{-4} cm/s) than matrix-supported samples (1×10^{-5} and 1×10^{-6} cm/s). In general, matrix-supported carbonate sediments composed of aragonite needles have higher permeabilities (1×10^{-5} cm/s) than matrix-supported sediments of low-magnesian calcite composed predominantly of coccoliths (1×10^{-6} cm/s). Analysis of scanning and transmission electron micrographs of carbonate and clayey sediments confirm the more open microstructure of carbonate sediments as opposed to the more evenly distributed but smaller sized clay micropores.

Introduction

The permeability of a sediment is a measure of the ease with which fluid flows through the sediment and of the number and size of the effective drainage paths available for fluid flow (Lambe, 1951; Bryant et al., 1975; Bennett et al., 1989). In the marine environment, the rate at which fluids leave the sediment under increasing overburden pressure controls the rate at which the sediment consolidates. Consolidation is the process whereby water is removed from the sediment by applying vertical pressure, which results in a realignment of grains and a more compact structure (Richards and Hamilton, 1967; Lambe and Whitman, 1969). Many physical properties, such as porosity and bulk density, are related to the degree of consolidation and are, therefore, indirectly controlled by the permeability of the sediment.

Ideally, permeability measurements should be made *in situ*. However, due to difficulties in obtaining *in situ* measurements in deep water, an alternate method is used to simulate *in situ* overburden pressures on the sample by applying a vertical load. The properties of interest are then measured under controlled conditions during the process of consolidation. As part of a larger study, the permeability and porosity of (a) periplatform sediments recovered from Exuma Sound and north of Little Bahama Bank, (b) samples of mixed carbonate and clay composition from Deep Sea Drilling Project (DSDP) Site 532 (Walvis Ridge), and (c) clays from DSDP Site 576 (northwest Pacific) were measured in a laboratory consolidation study. The purpose was to define the permeability of carbonate

sediments so that, in the absence of direct measurements, the permeability of sediments in similar environments but in different geographic locations can be estimated.

Background

The principle of effective stress (the difference between the total vertical stresses and pore-water pressure) asserts that effective stress, also called sediment or intergranular pressure, controls volume change and sediment strength behavior (Mitchell, 1976). Permeability and porosity are correlated with effective stress. Initially, both the pore fluid and sediment grains carry the overburden load as sedimentation occurs. As sediment consolidates with increasing load caused by continuous sedimentation, a realignment of grains and particles and a more compact structure results as the fluid is driven out of the sediment, and the sediment particles carry increasing portions of the load (Richards and Hamilton, 1967; Bryant and Bennett, 1988). Effective stress is the load carried by the sediment particles, or the total geostatic stress, minus the load-carrying contribution of the fluid and is expressed:

$$\sigma' = \sigma - \mu \,, \tag{1}$$

where σ' is the effective stress, σ is the total stress, and μ is the pore pressure. In normally consolidated sediments, the effective stress increases with increasing depth below the sediment-water interface. Many geotechnical properties depend on the strength, compressibility, and amount of pore water in the sediment. Therefore, as sediment consolidates, these geotechnical properties undergo change.

The coefficient of permeability (k), the rate of flow past a specified area, is calculated from:

$$k = c_{v50} * \gamma_w * m_{v50} \,, \tag{2}$$

where c_{v50} is the coefficient of consolidation, γ_w is the unit weight of water, and m_{v50} is the coefficient of volume change. Permeability is routinely measured by various techniques in the lab (Lambe, 1951; Enos and Sawatsky, 1980) and *in situ* (Bennett et al., 1989). In this study, permeability was measured in the laboratory using a variable head permeameter (see Lambe, 1951) for each consolidation load increment, beginning with a total vertical stress of 2 kg/cm^2 (19.6 kPa). In a saturated soil, water flow is laminar and Darcy's Law can be applied:

$$k = \frac{aL}{A(t_1 - t_0)} \log (h_0 - h_1) \,, \tag{3}$$

where a is the cross sectional area of the standpipe, L is the length of sediment, A is the cross sectional area of the sample, t_0 is the time when water in the standpipe is at h_0, t_1 is the time when water in the standpipe is at h_1, and h_0 and h_1 are the heads between which the permeability is determined.

Carbonate samples were examined with the scanning electron microscope (SEM) to identify fabric relationships and constituent particles and grains. The term particle or grain refers to a recognizable solid consisting of a clay mineral, rock-forming mineral, or biogenic debris ranging from colloidal to sand size. A grain may be a single unit or a composite of several units with recognizable form and internal structural integrity (Bennett et al., 1989). However, a grain behaves as a single unit under mechanical stress, such as consolidation. There are generally two basic size fractions. The smaller size fraction is referred to as matrix and matrix particles. The larger size fraction is composed of grains. The samples were classified as either matrix supported—grains floating within the matrix (Fig. 9.1); grain supported—the grains are in contact with each other (Fig. 9.2); or in several cases where the classification was difficult using SEM, as matrix supported with numerous grains. The distinction between matrix- and grain-supported sediments is important because it has been shown that matrix-supported and grain-supported samples will consolidate differently (Fruth et al., 1966; Rezak and Lavoie, 1990). In the sediments analyzed, the matrix material, generally a periplatform ooze, was of two main types: either predominantly a coccolith ooze or composed of a large proportion of aragonite needles (Fig. 9.3). Grains and particles

Figure 9.1. Scanning electron micrograph of a typical matrix-supported sediment. Matrix particles are coccoliths; no grains are present in this illustration.

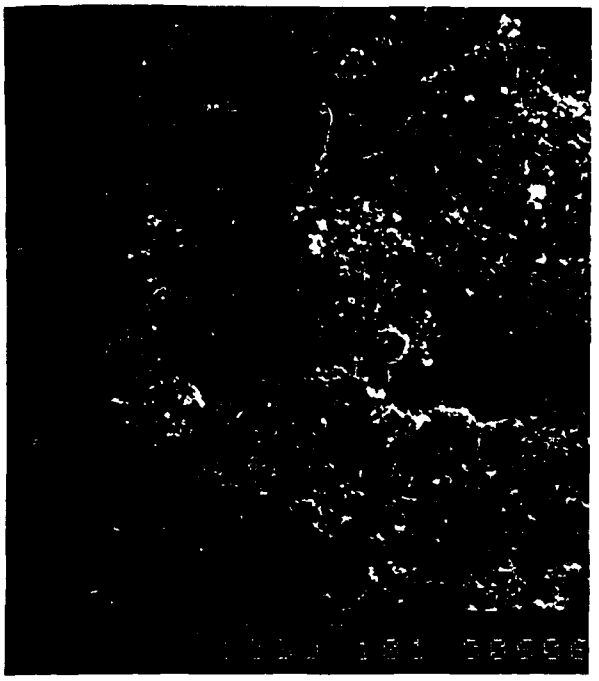

Figure 9.2. Scanning electron micrograph of a grain-supported sediment. The grains are in contact—very little matrix material is present. At higher magnification, viewing fields consist of skeletal portions of the grains.

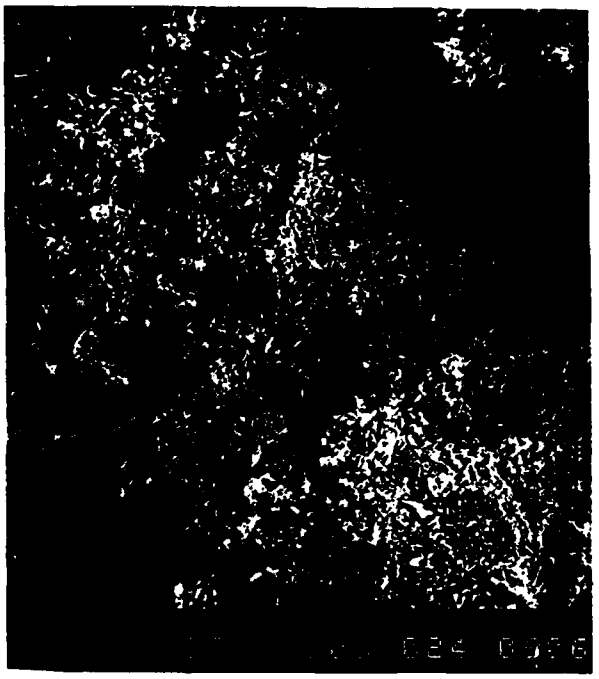

Figure 9.3. A typical periplatform sediment with an aragonite matrix for ES (sample id). The grains present are not in contact with each other.

that could not be positively identified as to origin because of breakage or other reasons were called "unidentifiable." Often, grains and particles would be identified as shell fragments because they had an aragonite needle structure or because they were planes of calcite.

The Bahamas were chosen as a source of carbonate sediments for this study, since they serve as a modern example of carbonate platforms and continental slope environments and are useful for interpreting the geological record. The northern Little Bahama Bank and Exuma Sound slopes sampled in this study (Fig. 9.4) represent extremes in carbonate slope development. Northern Little Bahama Bank, a gentle 2° to 3° slope, represents an accretionary, depositional slope, an early stage in the evolution of carbonate slopes. Exuma Sound, much steeper at 12° to 14°, represents the final erosional bypass stage of slope building (Schlager and Ginsburg, 1981). Sediment deposition on Exuma Sound is by turbidity currents that bypass the slope, depositing most of the sediments at the toe of the slope.

Along the continental slopes of Little Bahama Bank and Exuma Sound, the matrix material of the sediments is called a periplatform ooze. This is a fine-grained, clayey-silt-sized mix of platform-derived sediment and tests of planktonic organisms (Schlager and James, 1978). Compositional and grain-size differences between matrix sediment and grains (often turbidites) produce an initially heterogeneous sedimentary column. This heterogeneity is enhanced by differing rates of lithification between periplatform ooze and interbedded grains. The large proportion of metastable carbonates, aragonite and high-magnesian calcite, in the matrix ooze enhances the potential for dissolution and diagenetic alteration (Droxler et al., 1983; Mullins et al., 1985). This leads to an earlier induration of the periplatform matrix ooze compared with the normally coarser turbidite beds. The interbedded carbonate turbidite grains contain fewer metastable carbonate minerals. As a result, they resist lithification longer than the periplatform matrix material.

The carbonate sediments used in this study were highly variable with respect to constituent particle type and grain-size distribution, depending on water depths and depths at which the samples were recovered from below the seafloor. Samples recovered from Little Bahama Bank tended to be grain supported with larger constituent particles, such as pteropods (500 to 1000 μm) and foraminifers (50 to 100 μm). Samples from the slopes of Exuma Sound were more frequently matrix supported, with coccolith shields (2 to 4 μm) as the matrix particles.

For comparison between clays and carbonate sediments, data from pelagic red clays from DSDP Site 576 in the northwestern Pacific, and sediments from DSDP Site 532 on the flank of the Walvis Ridge (containing both clay and carbonate fractions) are presented. Illite forms the major

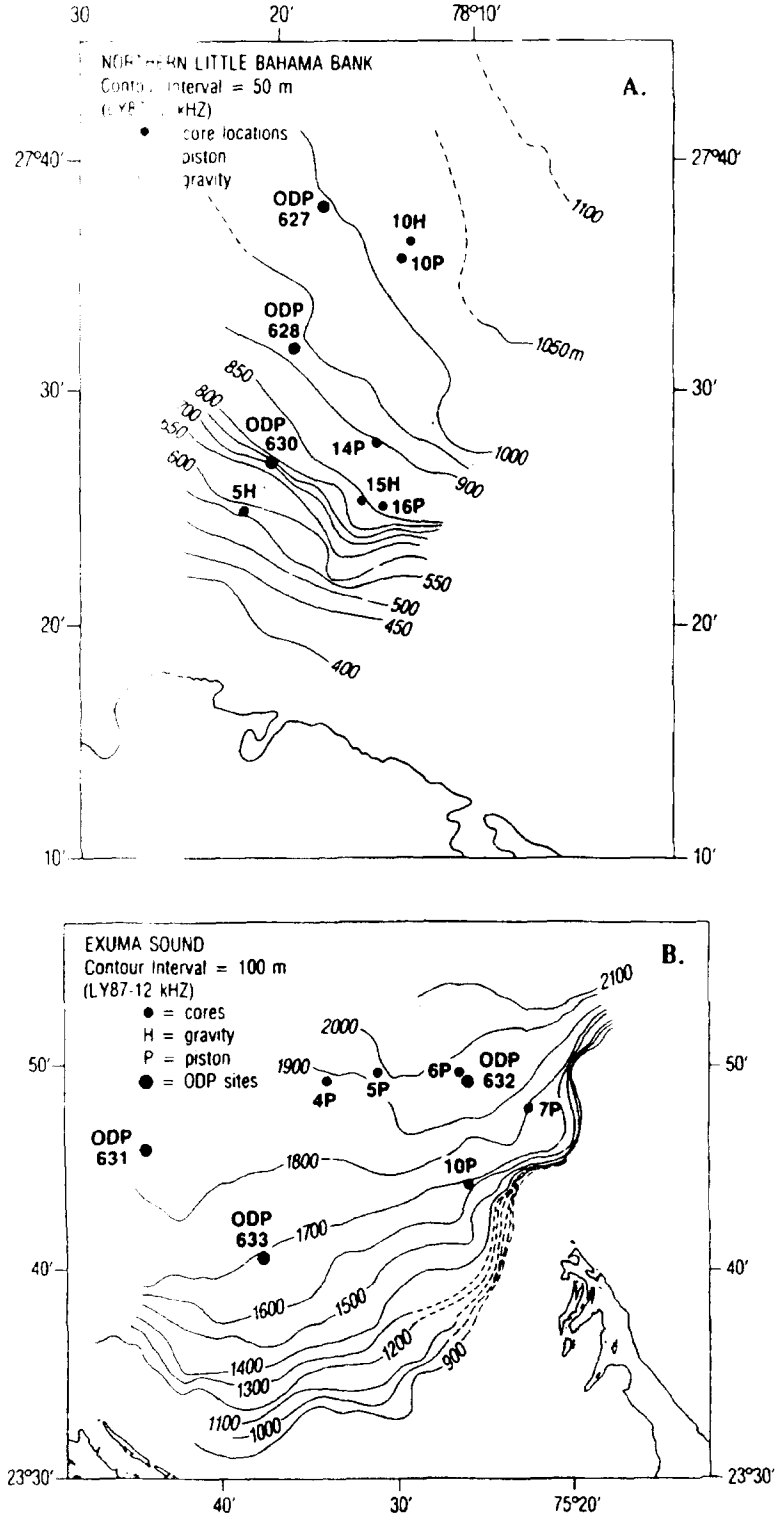

Figure 9.4. Core location maps. (A) Little Bahama Bank and (B) Exuma Sound. Ocean Drilling Program sites are also noted.

component (~ 50%) of the red clays from Site 576. Smectite (~ 10%) can be identified by its fleecy small particles and becomes increasingly important as subbottom depth increases. The red clays studied here had high water contents, high porosities and low bulk densities, and were carbonate free. Bennett et al. (1981) performed a clay fabric analysis of a red ay and described it as a complex structure of linked clay flocs with large intravoid spaces, which explains the high water contents and porosities. Figure 9.5 illustrates the complex structure of Site 576 red clays. The smectite particles (0.1 μm) are chained, leaving large void spaces, while the much larger illitic domains (0.5 to 3 μm) may act as grains in a matrix of smaller smectite particles. The illite grain shown in Figure 9.5 is atypical of the illites of the red clays which are usually fractured during the sectioning process (Bryant and Bennett, 88).

DSDP Site 532 on the Walvis Ridge is located under an area of intense upwelling. Sediments consist of a mix of terrigenous material derived from the shelf and slope and biogenic (predominantly carbonate) material derived from planktonic organisms in the overlying water column. The carbonate content of samples recovered from DSDP Site 532 ranges f om 18% near the surface (Pleistocene) to 70% at about 80 mbsf (late Pliocene). These samples are predominantly clay and silt ed, especially below 36 mbsf. The small sand fraction in the upper 36 m is probably composed of intact foraminifers. In the lower portions of the sediment column (especially at stresses greater than 2000 kPa), the resulting effective stress breaks the foraminifers into small fragments, causing the sand fraction to disappear.

Figure 9.5. Transmission electron micrograph of red clay from Deep Sea Drilling Project Site 576. Smectite particles are chained, leaving void spaces many times larger than themselves. The larger illite domains (0.5 to 3 μm) may act as grains in a smectite matrix. (Courtesy of P. J. Barker, NOAA/ SSC).

Results

Consolidation

The results of consolidation tests performed on the red clays from Site 576 and the periplatform carbonates from the Bahamas are presented as void ratio versus the log of effective stress (e log σ') curves, Figure 9.6a. The periplatform carbonate sediments have much lower initial void ratios than the red clays from Site 576 and are much less compressible. l ler similar loads, the red clays have higher initial void t. os, but final void ratios that are similar to the final void ratios of the periplatform carbonates. The e log σ' curves from Site 532 mixed sediments are presented separately in Figure 9.6b. As a group, these mixed sediments display a greater range of compressibility than the periplatform carbonates. In fact, when the e log σ' from the mixed sediment curves are laid over the red clay and periplatform carbonate curves, as in Figure 9.6c, it is evident that, except l ne one sample that is 70% carbonate, the e log σ' curves ar similar to those of the red clay samples.

Permeability

The periplatform slope sediments from the Bahamas tested in this study represent a fairly limited distribution of carbonates, yet they exhibit a wide range of permeabilities (Table 9.1). The wide range of permeabilities is evident when permeability is plotted against porosity, as in Figure 9.7. The periplatform samples from the Bahamas have an initial porosity between 56 and 65%, but the permeability measured during consolidation ranges over two orders of magnitude between 5×10^{-4} and 6×10^{-6} cm/s. Furthermore, the periplatform carbonates can be grouped into samples that are (a) generally matrix supported, with an initial permeability of about 1×10^{-5} and 1×10^{-6} cm/s, and (b) generally grain supported, with an initial permeability of 1×10^{-4} cm/s. Final permeability values, measured after consolidating the samples to ~4500 kPa, are 1 to 2 orders of magnitude lower, between 1×10^{-6} and 1×10^{-7} cm/s. In contrast, the red clays from Site 576 display a greater degree of permeability reduction over the same range of overburden pressures. Initial and final porosity is higher than the carbonate samples, yet the final permeability for the red clays

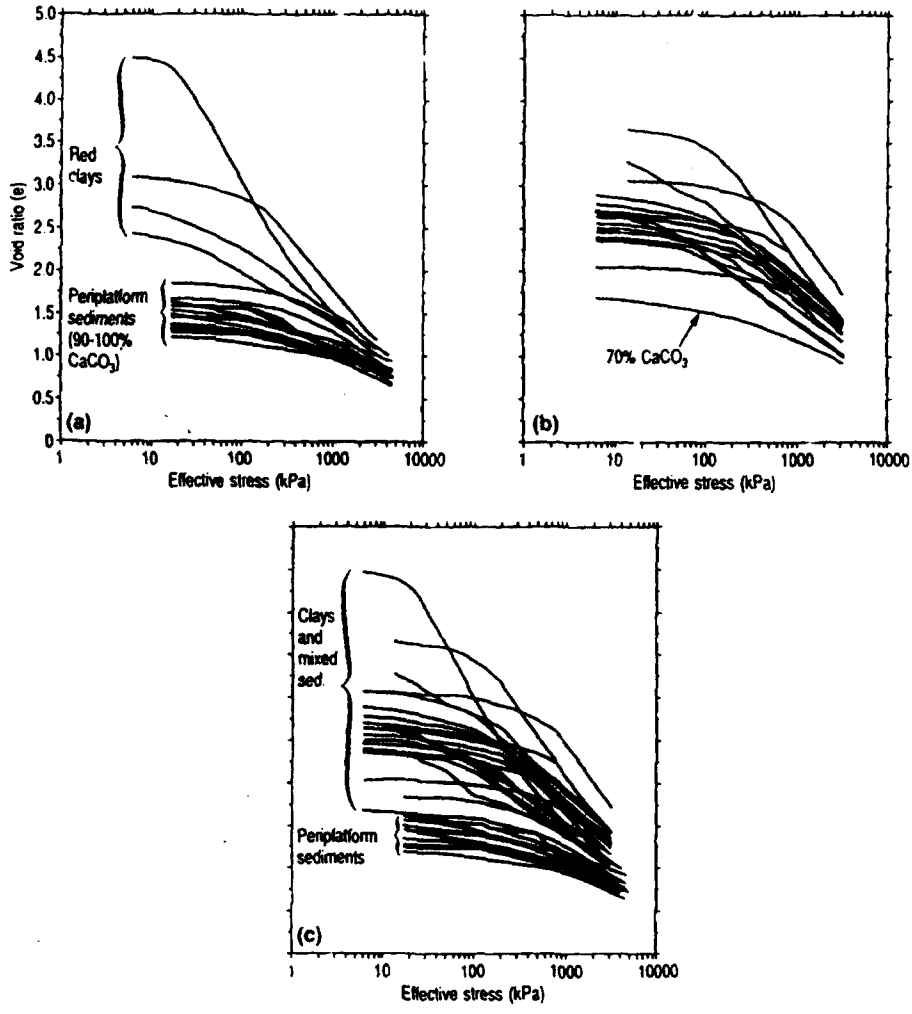

Figure 9.6. Three e log σ' curves for (a) red clays for DSDP Site 576 and periplatform carbonate sediments from the Bahamas; (b) sediment from DSDP Site 532 containing a mixture of carbonate and clay sediment. When results from all sediments are plotted together (c), periplatform sediments consolidate less than red clays (Site 576) and mixed sediments (Site 532), except for the one sediment containing 70% carbonate, which displays consolidation behavior similar to that of the periplatform carbonates.

is about 1×10^{-8} cm/s, an order of magnitude lower than for the periplatform carbonates.

Results from permeability testing of the mixed clay and carbonate sediments from Site 532 are presented separately in Figure 9.7b. Rather than forming a continuum of values that fall between those of the periplatform carbonates and red clays, the mixed clay and carbonate sediments from Site 532 display behavior similar to that of the clays. Initial and final porosities are higher than those of the periplatform carbonates. Initial permeability values are similar to those for both clays and carbonates, 1×10^{-4} and 1×10^{-5} cm/s, but the mixed sediments display the same large reduction in permeability as do the clays; final permeability for the mixed sediments is about 1×10^{-8} cm/s.

Discussion

A number of factors affect permeability, among them the fabric, or the orientation of particulate grains and void spaces. It is thought that fabric is altered by application of pressure (Terzaghi, 1940; Hathaway and Robertson, 1961; Fruth et al., 1966; Shinn et al., 1977; Shinn and Robbin, 1983; Lavoie, 1985; Bennett et al., 1989). Clays in the unconsolidated condition typically have high void ratios and high porosities due to the structural integrity of the domains. Under consolidation, the fabric changes considerably, various domains become aligned, and a considerable reduction in the void space and porosity occurs. Figures 9.8a and b show an illitic clay from the Sigsbee Abyssal Plain. In Figure 9.8a, illite is easily identified by

Table 9.1. Results of induced effective stresses between 17 and 4500 kPa.

Sample ID	Description	$n_{(i)}$	$n_{(f)}$	$k_{(i)}$ (cm/s)	$k_{(f)}$ (cm/s)	$e_{(i)}$	$e_{(f)}$
Periplatform Carbonates - Bahamas							
ES4P-1	Matrix-supp	0.56	0.44	6.64×10^{-6}	1.75×10^{-6}	1.27	0.78
ES4P-2	Matrix-supp	0.65	0.55	3.76×10^{-6}	5.40×10^{-7}	1.85	1.21
ES4P-3	Matrix-supp	0.56	0.46	3.72×10^{-6}	2.59×10^{-7}	1.27	0.84
ES4P-4	Matrix-supp	0.59	0.41	2.53×10^{-6}	4.57×10^{-7}	1.45	0.76
ES5P-2	Matrix-supp	0.59	0.45	4.21×10^{-6}	6.94×10^{-7}	1.46	0.82
ES5P-3	Matrix-supp	0.48	0.19	1.13×10^{-5}	5.80×10^{-7}	1.82	1.29
ES5P-4	Matrix-supp	0.55	0.35	3.61×10^{-6}	3.30×10^{-7}	1.85	1.29
ES5P-5	Matrix-supp	0.61	0.39	6.65×10^{-6}	3.09×10^{-7}	1.58	0.64
ES6P-2	Matrix-supp	0.63	0.46	4.40×10^{-5}	2.43×10^{-6}	1.67	0.85
ES6P-3	Matrix-supp	0.58	0.43	1.84×10^{-6}	8.00×10^{-7}	1.37	0.74
ES6P-4	Matrix-supp	0.57	0.42	2.50×10^{-6}	5.47×10^{-7}	1.33	0.72
ES7P-1	Matrix-supp	0.61	0.43	2.37×10^{-6}	6.89×10^{-7}	1.56	0.76
ES7P-2	Matrix-supp	0.59	0.46	7.66×10^{-5}	3.01×10^{-7}	1.45	0.85
ES7P-4	Matrix-supp	0.55	0.43	9.41×10^{-7}	3.92×10^{-7}	1.21	0.74
ES10P-3	Matrix-supp	0.57	0.42	5.25×10^{-5}	3.72×10^{-6}	1.33	0.72
ES10P-4	Matrix-supp	0.60	0.49	1.41×10^{-5}	1.87×10^{-7}	1.52	0.94
LBB10P-1	Grain-supp	0.57	0.38	4.82×10^{-4}	1.20×10^{-5}	1.30	0.63
LBB14P-1	Grain-supp	0.62	0.40	5.64×10^{-4}	3.00×10^{-7}	1.63	0.67
LBB15H-1	Matrix-supp (arag)	0.61	0.51	2.72×10^{-5}	7.50×10^{-7}	1.58	1.03
LBB16P-1	Matrix-supp (arag)	0.55	0.48	2.77×10^{-3}	2.54×10^{-6}	1.33	0.79
LBB16P-2	Grain-supp	0.58	0.49	5.53×10^{-4}	4.11×10^{-4}	1.47	0.55
Site 576 - North Pacific							
1	Red Clay	0.70	0.47	4.22×10^{-5}	2.96×10^{-9}	2.43	0.87
2	Red Clay	0.73	0.52	2.84×10^{-4}	1.29×10^{-9}	2.73	1.09
3	Red Clay	0.76	0.54	2.19×10^{-6}	3.03×10^{-9}	3.09	1.19
4	Red Clay	0.82	0.50	2.71×10^{-5}	8.79×10^{-9}	4.49	1.00
Site 532 - Mixed Clays and Carbonates - Walvis Ridge, South Atlantic							
% Carbonate							
18		0.73	0.51	4.67×10^{-7}	4.15×10^{-9}	2.06	1.42
31		0.73	0.69	1.60×10^{-6}	1.30×10^{-7}	2.70	2.24
35		0.63	0.49	5.60×10^{-7}	5.33×10^{-9}	1.69	0.94
35		0.73	0.59	1.60×10^{-6}	6.74×10^{-8}	2.65	1.44
37		0.71	0.58	1.81×10^{-6}	1.78×10^{-7}	2.41	1.37
40		0.72	0.54	7.02×10^{-7}	4.01×10^{-8}	2.57	1.19
40		0.73	0.54	1.18×10^{-6}	6.27×10^{-8}	2.66	1.17
41		0.79	0.59	1.92×10^{-5}	1.34×10^{-8}	2.90	1.30
43		0.72	0.59	9.10×10^{-6}	1.27×10^{-7}	3.68	1.45
44		0.73	0.59	5.50×10^{-5}	1.16×10^{-8}	2.73	1.04
46		0.74	0.57	2.20×10^{-6}	1.19×10^{-8}	2.47	1.05
49		0.73	0.59	1.30×10^{-5}	9.19×10^{-8}	2.73	1.43
49		0.77	0.66	6.70×10^{-6}	2.52×10^{-7}	3.29	1.98
54		0.75	0.58	4.87×10^{-7}	8.55×10^{-9}	3.07	1.36
55		0.72	0.60	1.60×10^{-6}	6.61×10^{-8}	2.51	1.47
58		0.74	0.56	1.30×10^{-5}	4.68×10^{-8}	2.80	1.26
60		0.60	0.53	6.40×10^{-7}	5.19×10^{-8}	1.50	1.11
64		0.67	0.59	3.23×10^{-5}	4.06×10^{-8}	2.40	1.02
64		0.70	0.53	6.03×10^{-6}	7.35×10^{-9}	2.37	1.11
69		0.70	0.53	8.60×10^{-6}	1.95×10^{-7}	2.52	1.41
70		0.71	0.51	1.74×10^{-4}	2.72×10^{-6}	2.36	1.13

Legend:
n = porosity, k = permeability, e = void ratio, (i) = initial, (f) = final
ES denotes cores recovered from Exuma Sound
LBB denotes cores recovered from Little Bahama Bank

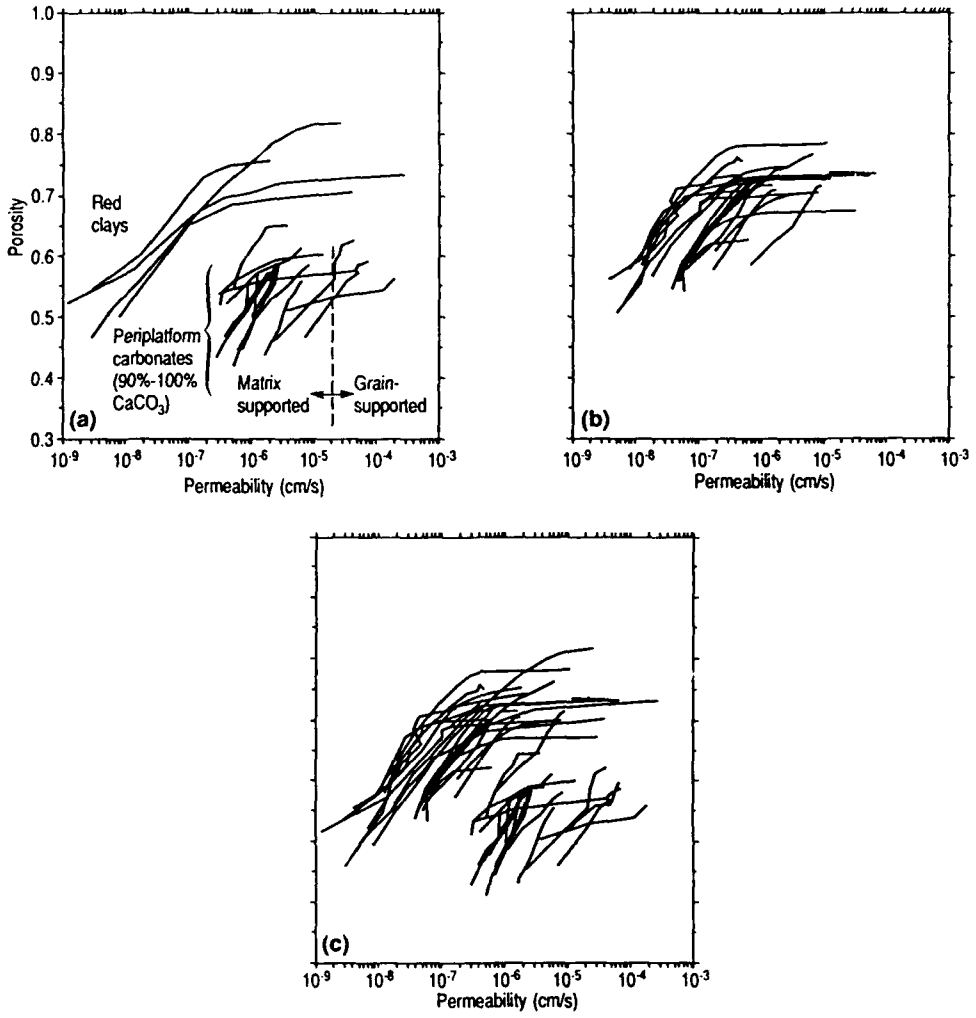

Figure 9.7. Permeability as a function of porosity is distinctly different between red clays and periplatform carbonates (a). The reduction in permeability is greater in red clays than in periplatform sediments for a given effective stress. Porosity in the unconsolidated state is higher for red clays than periplatform sediments. In addition, grain-supported periplatform sediments have higher initial permeabilities than matrix-supported sediments. Permeability for Site 532 mixed sediments (b) is very similar to that of red clays. When permeability versus porosity for all sediment is plotted (c), the mixed sediments (Site 532) and red clays (Site 534) display high porosities and a greater reduction in permeability during consolidation than periplatform carbonates.

fractured nature (fractillites were first described in connection with the Pacific red clays; Bryant and Bennett, 1988) and surrounds voids several times the size of the individual illite particles. The void spaces are about 4-μm long with a width:length ratio of about 1:4 to 1:2. After a load of 392 kPa was applied during the consolidation testing, which was a fraction of the total load of 4500 kPa normally applied, the illite grains are well oriented. At this point the void spaces are much smaller and more elongated. They are about 1 to 3 μm long and have width:length ratios between 1:2 to 1:10 (Fig. 9.8b).

In contrast, examination of SEM micrographs, before and after the consolidation of periplatform sediments, reveals slight differences in fabric that are difficult to see with the eye (Figs. 9.9a, b). Examination of void spaces using the LaMont Image analysis system demonstrated a small reduction in void spaces in the matrix-supported periplatform sediments. In other samples, the void size appeared not to have changed significantly (Rezak and Lavoie, 1990). These visual impressions are supported by the e log σ' curves that illustrate the tendency of the periplatform carbonates to consolidate less than the red clays. It is reasonable, since the periplatform

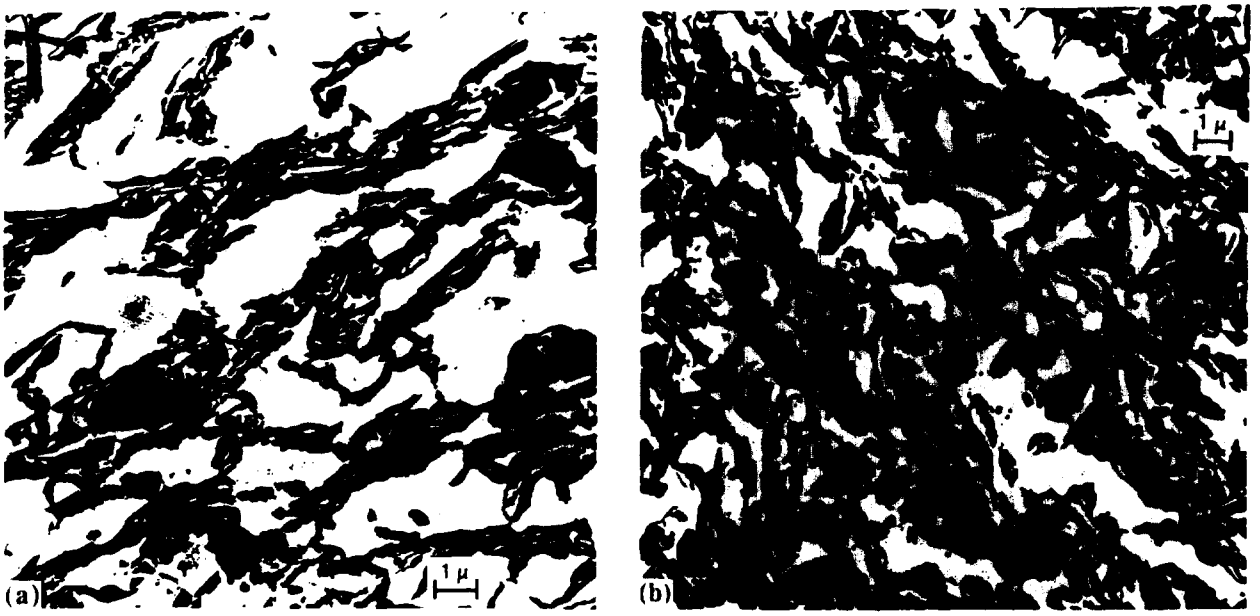

Figure 9.8. Transmission electron micrograph of an illitic clay for the Sigsbee Abyssal Plain. (a) In the unconsolidated state, void spaces are large in comparison with illite particles. (b) After consolidation to 392 kPa, void spaces are much smaller than in the unconsolidated state, and a distinct lineation of the fabric is evident. (Courtesy of E.A. Bowles, NOARL, SSC)

carbonates consolidate less and display less change in void size, that they also have less reduction in permeability than the red clays.

The differences in the initial permeability between the periplatform carbonates can best be understood by examining the fabric and con tituent particles. High permeability seems to be a function of both grain size and aragonite needle content. There appears to be a division of the initial permeability into two groups. Grain-supported samples had the highest initial permeability, on the order of 1×10^{-4} cm/s, and matrix-supported samples had initial permeabilities on the order of 1×10^{-5} and 1×10^{-6} cm/s. Matrix-supported samples with aragonite needle matrices had higher initial permeabilities than the samples with coccolith matrix particles. For example, LBB 14P-1, a grain-supported pteropod ooze, has an initial permeability of 5.57×10^{-4} cm/s. LBB 16P-1, almost entirely composed of aragonite needles with only a few floating grains, had an initial permeability of 2.77×10^{-5} cm/s. Another matrix-supported sample with coccolith shields as matrix particles, ES 4P-2, had an initial permeability of 3.72×10^{-6} cm/s. The difference in initial permeability between the two matrix-supported samples can be found in the particular types of matrix particles. Both the aragonite needles and coccolith shields are of similar size (3 to 4 μm); however, the aragonite needles have only one long axis, while the coccoliths are plate-like and have radial axes of similar length in any direction. The void spaces in the two matrix types are, therefore, very different. The needles form an open, highly porous permeable fabric, while the coccolith shields result in a more complex matrix having small pores and restricted fluid pathways. In contrast to the matrix-supported samples, the grain-supported samples tended to be very sandy. Although there was undoubtedly matrix material plugging pore spaces between the grains, the pore throats were evidently protected to a considerable extent by the overall size of the pores formed by the rounded surfaces of the grains in contact.

The high permeability of aragonite and sand-rich sediments is not necessarily predicted by porosity. The initial porosity of this sediment was between 55 and 65% and between 47 and 53% after consolidation (Table 9.1). When permeability was plotted as a function of porosity, correlation coefficients were low; for grain-supported sediments, $r = 0.46$, and for matrix sediments, $r = 0.42$. Laboratory porosity measurements reflect total porosity, including intraparticle porosity. Often sediments that contain coccolith matrix particles and foraminifer grains have a high proportion of fluid contained within the grains that contributes little to effective fluid flow, since the pore spaces are not necessarily connected. The silicious dinoflagellate depicted in Figure 9.9a illustrates intraparticle porosity within the matrix. As the porosity is reduced, the permeability may or may not be reduced, depending on whether the reduction in porosity is in the interconnected pore spaces or in the intraparticle space. In contrast, the aragonite needle samples have little intraparticle porosity; most of the pore spaces act as fluid conduits. The

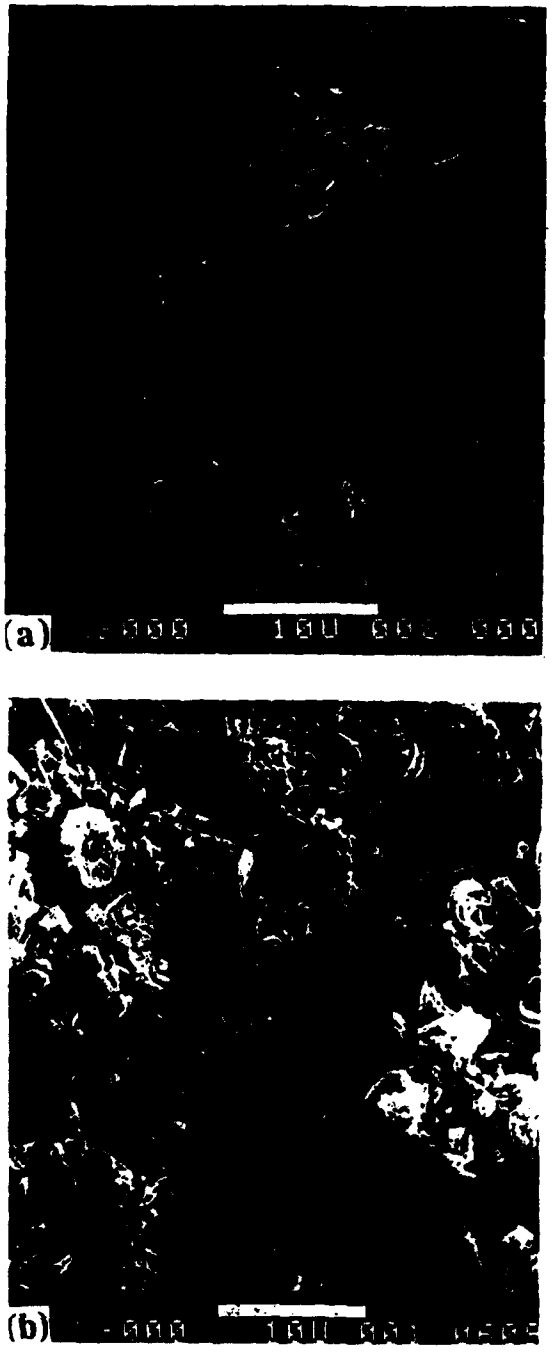

Figure 9.9. Scanning electron micrographs of ES (a) in the unconsolidated state and (b) after consolidating to 4500 kPa. Little fabric change has occurred during consolidation. Calcareous dinoflagellate cyst illustrates intraparticle porosity in matrix particles.

decrease in porosity after consolidation reflects only the constriction of interparticle void spaces as the grains become more tightly packed. It was expected that the permeability would decrease proportionally. However, permeability is actually a function of the size of the pore throats, or the effective passageways. If the pore throat size is small compared to the overall pore size, a reduction in overall porosity may reduce the overall pore size without reducing pore throat size. In this case, where overall porosity is reduced without a reduction in size of the pore throats, permeability is less affected. Thus, without knowing fabric and particle type, porosity may not be a good predictor of permeability in carbonate sediments.

When the sediment is grain-supported, the pore spaces within the matrix are protected from constriction, at least until grain crushing occurs. When the sediment is matrix-supported, considerable volume change may occur as the matrix consolidates and pore spaces become reduced, which lowers permeability. In periplatform oozes, there was very little difference in the total amount of consolidation between grain-supported and matrix-supported samples; however, considerable grain crushing was observed, especially in grain-supported samples such as ES 6P-1 (top) and LBB 16P-1. Figure 9.10 illustrates typical grain crushing as observed in SEM micrographs after consolidation. The foraminifer grains contain significant amounts of intraparticle water, which is released as the grains are crushed. Therefore, a sediment that has undergone considerable grain crushing should exhibit a lower porosity than one that has not. Porosities at 4500 kPa for the periplatform samples are all very similar, generally ranging between 35 and 45% with no apparent differences between matrix- and grain-supported samples. Grain crushing of foraminifers (or equally hollow particles) may have occurred in the grain-supported samples in an amount such that the volume and porosity reduction equals that of matrix-supported samples.

In general, the mixed sediments that contain large proportions of carbonate material (18 to 70% calcium carbonate) from Site 532 display consolidation characteristics and permeability values more similar to the red clays than to the periplatform sediments. The matrix of the mixed sediments is composed of smaller clay mineral particles, while the larger carbonate fraction forms the grains. The permeability of sediments is controlled by the matrix, and in particular the pore throats of the clay mineral fraction. Thus, in a mixed sediment composed of clays and carbonates, the permeability is controlled by the clay material. This holds true for samples that contain up to 70% calcium carbonate. The only exception in this group was the sample containing 70% calcium carbonate. That carbonate displayed consolidation characteristics and permeability values typical of a matrix-supported periplatform carbonate sediment. The percentage of calcium carbonate in a sediment must be greater than 60% calcium carbonate before permeability is appreciably affected by the presence of a carbonate fraction.

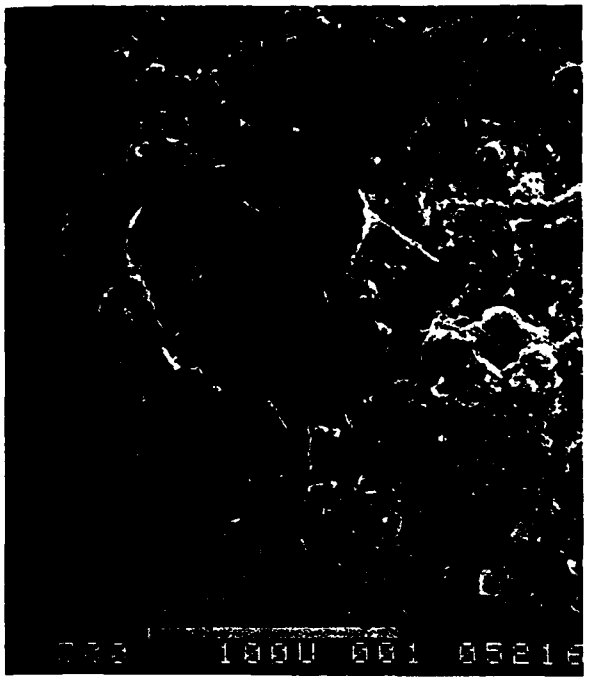

Figure 9.10. Typical grain crushing observed in grain-supported sediments after 2000 kPa has been applied.

Conclusions

1. Carbonates with greater than 90% calcium carbonate, such as the Bahamian periplatform sediments, have lower porosities and are much less compressible than either red clays (DSDP Site 576) or mixed clay and carbonate sediments (DSDP Site 532).
2. The permeability of periplatform carbonates is similar to that of red clays and clay and carbonate mixtures in the unconsolidated state. During consolidation, the reduction in permeability is much less in the periplatform sediments than in either red clays or mixed clay and carbonate sediments. Mixed clay and carbonate sediments behave in a fashion similar to red clays until a carbonate content of 70% or greater is reached.
3. Permeability is controlled by the matrix particles. In the case of mixed clays and carbonate sediments, the matrix is composed of clay minerals; hence, its permeability behavior is similar to that of clay sediments. In the case of periplatform sediments, samples composed of aragonite needles have the highest permeability, samples with coccolith matrices have the lowest. Grain-supported sediments tend to have higher permeabilities because the pore throats are protected by the grains and are less affected by consolidation than they are in matrix-supported sediments. Carbonate samples with grain-supported fabrics display slight changes in permeability until loads sufficient to cause grain crushing are reached. At that point, permeability suddenly decreases.
4. In carbonate sediments, total porosity alone is not a good predictor of permeability. Intraparticle porosity may not be interconnected with interparticle porosity and may not contribute to permeability. Porosity in sediment with aragonite needle matrices is different from porosity in sediments with matrices consisting of platey grains and a different geometry.
5. Permeability of sediments examined ranges between 2.77×10^{-3} and 8.00×10^{-7} cm/s for periplatform carbonates, between 2.84×10^{-4} and 8.79×10^{-9} cm/s for red clays, and between 1.74×10^{-4} and 8.55×10^{-9} cm/s for mixed clay and carbonate sediments.

Acknowledgments

The authors thank Dr. Richard Rezak of Texas A&M University and Mr. Dennis Lavoie of NOARL for their help with the scanning electron microscopy. We especially appreciate Mr. Dave Young of NOARL and Ms. Samantha Breeding of Planning Systems, Inc., for their support with the fabrication of laboratory equipment and the many sample analyses. We also acknowledge the helpful suggestions of Dr. Roy Wilkins of the University of Hawaii, Dr. Richard Bennett of NOARL, and Dr. Frank Rack of Texas A&M University. This work was supported by NOARL's basic research program, directed by Mrs. Halcyon Morris, NOARL Program Element 0601153N.

References

Bennett, R.H., K.M. Fischer, D.L. Lavoie, W.R. Bryant, and R. Rezak, 1989. Porometry and fabric of marine clay and carbonate sediments: determinants of permeability. Marine Geology, v. 89, p. 127-152.

Bryant, W.R. and R.H. Bennett, 1988. Origin, physical, and mineralogical nature of red clays: The Pacific Ocean Basin as a model. Geo-Marine Letters, v. 8, p. 189-249.

Bryant, W.R., W. Hottman, and P. Trabant, 1975. Permeability of unconsolidated and consolidated marine sediments, Gulf of Mexico. Marine Geotechnology, v. 1, p. 1-14.

Droxler, A.W., W. Schlager, and C.C. Whallon, 1983. Quaternary aragonite cycles and oxygen-isotope record in Bahamian carbonate ooze. Geology, v. 11, p. 235-239.

Eberli, G.P., 1988. Physical properties of carbonate turbidite sequences surrounding the Bahamas—implications for slope stability and fluid movements. In: Austin, J.A., W. Schlager and others (eds.), Proceedings, *Ocean Drilling Program, Scientific Results, 101*, College Station, TX, p. 305-314.

Enos, P. and L.H. Sawatsky, 1980. Pore networks in Holocene carbonate sediments. Journal of Sedimentary Petrology, v. 51, p. 961-981.

Etris, E.L., D.S. Brumfield, R. Ehrlich, and S.J. Crabtree, 1988. Relations between pores, throats and permeability: a petrographic / physical analysis of some carbonate grainstones and packstones. Carbonates and Evaporites, v. 3(1), p. 17-32.

Fischer, K.M., H. Li, R.H. Bennett, and W.A. Dunlap, 1990. Calculation of permeability coefficients of soils and marine sediments. Environmental Software, v. 5, p. 29-37.

Fruth, L.S., Jr., G.R. Omre, and F.A. Donath, 1966. Experimental compaction effects in carbonate sediments. Journal of Sedimentary Petrology, v. 36(3), p. 747-754.

Hamilton, E.L., 1976. Variations of density and porosity with depth in deep-sea sediments. Journal of Sedimentary Petrology, v. 46(2), p. 280-300.

Hathaway, J.C. and E.C. Robertson, 1961. Microtexture of artificially consolidated aragonitic mud. USGS Prof. Paper, 424C, p. 301-304.

Lambe, T.W., 1951. Soil Testing for Engineers. John Wiley & Sons, Inc., New York, 165 p.

Lambe, T.W. and R.V. Whitman, 1969. Soil Mechanics. John Wiley & Sons, Inc., New York, 553 p.

Lavoie, D.L., 1988. Geotechnical properties of sediments in a carbonate-slope environment: Ocean Drilling Program Site 630, Northern Little Bahama Bank. In: Austin, J.A., W. Schlager and others (eds.), Proceedings, Ocean Drilling Program, Scientific Results, 101, College Station, TX, p. 315-326.

Mitchell, J.K., 1976. Fundamentals of Soil Behavior. John Wiley & Sons, Inc., New York, 422 p.

Mullins, H.T., L.S. Land, W.W. Wise, Jr., D.I. Seigel, P.M. Masters, E.J. Hinchey, and K.R. Price, 1985. Shallow subsurface diagenesis of Pleistocene periplatform ooze: Northern Bahamas. Sedimentology, v. 32, p. 480-494.

Rezak, R. and D.L. Lavoie, 1990. Consolidated related fabric changes in periplatform sediments. Geo-Marine Letters, v. 10, p. 101-109.

Richards, A.F. and E.L. Hamilton, 1967. Investigation of deep-sea cores, III. Consolidation. In: Richards, A.F. (ed.), Marine Geotechnique, University of Illinois Press, p. 93-117.

Schlager, W. and R.N. Ginsburg, 1981. Bahama carbonate platforms—the deep and the past. Marine Geology, v. 44, p. 1-24.

Schlager, W. and N.P. James, 1978. Low-magnesian calcite limestones forming at the deep-sea floor, Tongue of the Ocean, Bahamas. Sedimentology, v. 25, p. 675-702.

Shinn, E.A., R.B. Halley, J.H. Hudson, and B.H. Lidz, 1977. Limestone compaction: an enigma. Geology, v. 5, p. 21-24.

Shinn, E.A. and D.M. Robbin, 1983. Mechanical and chemical compaction of fine-grained shallow-water limestones. Journal of Sedimentary Petrology, v. 53, p. 595-618.

Terzaghi, R.D., 1940. Compaction of lime mud as a cause of secondary structure. Journal of Sedimentary Petrology, v. 10(2), p. 78-90.